Pressure Tuning of Solvent Relaxation Time for the Excited Intramolecular Charge-Transfer Kinetics in 4-(*N*,*N*-Dimethylamino)triphenylphosphine in Alcohol

Noritsugu Kometani, Okitsugu Kajimoto, and Kimihiko Hara*

Division of Chemistry, Graduate School of Science, Kyoto University, Sakyo-ku, Kyoto 606-01 Japan

Received: December 16, 1996; In Final Form: March 12, 1997[⊗]

The dynamic solvent effect on the excited state intramolecular charge-transfer (ICT) reaction of 4-(*N*,*N*-dimethylamino)triphenylphosphine (DMATP) in alcohol solvents is examined by a high-pressure method. In order to deduce the solvation effect on the ICT reaction of DMATP, the picosecond time-dependent Stokes shift (TDSS) of coumarin 153 (C153) in alcohols is measured as a function of pressure. The resulting high-pressure solvent relaxation time (τ_s) is in excellent agreement with the longest longitudinal relaxation time (τ_L) of alcohols from low-temperature sources. In the low-viscosity region at low pressures, the rate of the ICT formation correlates with τ_s (or τ_L), while in the high viscosity region at high pressures, it becomes noticeably faster than τ_s (or τ_L).

Introduction

Understanding how chemical reactions are affected by solvation has long been a topic of interest in physical chemistry.[1] Recent emphasis in this area has centered around dynamic aspects of the solvent influence, especially with respect to intramolecular charge-transfer (ICT) reactions in the excited state.[2]

Instantaneous electrical excitation of a flexible aromatic molecule breaks down the resonance stabilization in the ground state. As the result, the structure of the ground state transforms to a new stable one in the excited state. If a large-amplitude intramolecular twisting motion is required for the transformation to occur, a smaller rate constant will be expected with increasing solvent viscosity. For the so-called "twisted intramolecular charge-transfer (TICT) state" formation in the excited state, the charge-transfer state process is considered as accompanied by a large-amplitude twisting motion.[3] In the case of a typical TICT state forming molecule, (*N*,*N*-dimethylamino)benzonitrile (DMABN), however, a less significant solvent viscosity effect has been detected,[4,5] contrary to the early expectation.[6]

We have used the high-pressure method to change the solvent viscosity and verified the viscosity dependence of various TICT state forming reactions.[7−9] The application of high pressure causes a change in solvent viscosity greatly and continuously in a *single* solvent without altering the solvation structure to any significant extent.

We have been studying the dynamic solvent effect on the excited state ICT reaction of 4-(*N*,*N*-dimethylamino)triphenylphosphine (DMATP) in linear alcohol solvents. A preliminary account of the viscosity dependence of the ICT reaction of DMATP was presented in ref 9. In order to understand further the role of solvent dynamics in the ICT reaction of DMATP, the accurate time scale of solvent relaxation at high pressure is needed. In the discussions of the previous papers,[8,9] the longitudinal relaxation time (τ_L), which is provided by a dielectric continuum model, has been used to gauge the solvent dynamics pertinent to ICT reactions. However, there is a question whether τ_L actually denotes the real time-scale for solvent relaxation. Recent time-dependent Stokes shift (TDSS) studies of probe molecules in polar solvents have revealed the solvation time scales. Such TDSS measurements at atmospheric pressure have been carried out recently by a number of groups.[10−14].

In this paper we are concerned with the effect of pressure on TDSS to provide the more definitive understanding how the ICT dynamics of DMATP are affected by the solvent dynamics. To probe the solvation dynamics, we employ a single solute, coumarin 153 (C153), which has already been used extensively as an ideal solvation dynamics probe.[10−14] By using the solvent relaxation times at high pressures, the solvent viscosity dependence of the ICT formation constant (k_{ICT}) is analyzed and the "pressure tuning effect" [8,9] of solvent relaxation time on the ICT reaction is clearly verified.

Experimental Section

The purified sample of DMATP was provided by Prof. W. Rettig of Humboldt University and was used as received. The probe molecule C153 is a laser grade material from Exciton. They showed no signs of fluorescence impurity within the wavelength region examined.

Picosecond time-resolved fluorescence spectra of DMATP and C153 were measured by the method of time-correlated single-photon counting (TCSPC) at high pressures up to 490 MPa in four linear alcohol solvents (ethanol, 1-propanol, 1-butanol, and 1-pentanol) at 303 K. The high-pressure optical cell[15] and the experimental arrangement of the laser system[16] were reported previously.

The second and third harmonic radiation of a mode-locked Ti:sapphire laser (Spectra-Physics, Tsunami Model 3950) was used as the excitation light source. The excitation wavelengths were 410 nm for C153 and 280 nm for DMATP. The Ti:sapphire laser, which was pumped by a cw argon ion laser, produced 840 nm light pulsed of 1.5 ps duration and had a repetition rate of 82 MHz. The pulse repetition rate was decreased to 8.2 MHz by using an electrooptic light modulator (Con Optic, Model 1305). A Hamamatsu R2809-02u microchannel plate (MCP) photomultiplier tube was used for detection. The overall instrument response function has an FWHM of approximately 30 ps at the excitation wavelength.

Results and Discussion

Dynamic Solvent Effect on CT Reaction of DMATP. In order to obtain the information of the dynamic solvent effect on the excited state intramolecular charge-transfer (ICT) formation kinetics of DMATP in alcohol solution, we investigate the

* Author to whom correspondence should be addressed (e-mail address: hara@kuchem.kytoto-u.ac.jp).

⊗ Abstract published in *Advance ACS Abstracts,* June 1, 1997.

S1089-5639(96)04078-9 CCC: $14.00

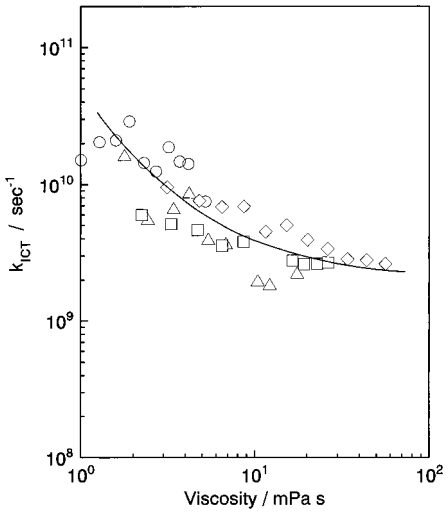

Figure 1. Plot of k_{ICT} against solvent viscosity (○, ethanol; △, 1-propanol; □, 1-butanol; ◇, 1-pentanol).

population decay of the locally excited (LE) state using the time-resolved emission spectroscopy at high pressures. The steady state emission spectrum of DMATP in alcohol at atmospheric pressure (= 0.1 MPa) is composed of an LE state component for wavelengths shorter than 370 nm and a CT state component at a wavelength around 470 nm.[9] The decay curves of the LE emission cannot be reproduced by single-exponential fittings. Instead, these LE decay curves are successfully described by the multiexponential equation

$$I_\lambda(t) = \int_{-\infty}^{t} [\sum A_i \exp(t-\tau)/\tau_i] G(\tau)\, d\tau \qquad (1)$$

where A_i and τ_i are the amplitudes and the time constants for the ith component of a multiexponential fit. $G(\tau)$ is the instrumental response function (IRF), which is determined by scattering the excitation pulse into the detecting high-pressure system. Thus, eq 1 expresses the intensity $I_\lambda(t)$ at a given wavelength λ as a convolution of the instrumental response and a multiexponential decay. Note that the τ_i values are independent of λ. Typically, triple-exponential fits were needed to accurately reproduce the emission decays on the blue edges of the spectrum, although in some cases the decays across the emission spectrum could be adequately fit using a biexponential function. The multiexponential behavior of the LE state decay leads to a conclusion that the simple two-state model is not adequate for the present ICT reaction scheme.

By using the values of A_i and τ_i obtained from the fitted curves, the average lifetime τ_a is determined.

$$\tau_a = \sum_i \tau_i A_i \qquad (2)$$

Here, we find that the contribution of the $S_1 \rightarrow S_0$ deactivation process is ruled out according to the following observations. (i) The contribution of the longest component (i.e., A_3 in eq 2) is less than 10%. (ii) The longest time constant (τ_3) becomes longer with pressure.[17] Consequently, the τ_a values imply the kinetics within the ecited state, so that by the inverse of τ_a, the average rate constant of the ICT state formation (k_{ICT}) is defined as follows:

$$k_{ICT} = (\tau_a)^{-1} \qquad (3)$$

In Figure 1, the k_{ICT} values of DMATP determined by such procedure in the series of compressed linear alcohols from ethanol to 1-pentanol are plotted as a function of solvent viscosity (η) in double logarithmic scale. This plot covers the viscosity range from 1.003 to 56.3 mPa s. The high-pressure viscosity data were obtained by interpolation or extrapolation of literature data[18,19] through polynomial fittings. We can see in Figure 1 that the viscosity dependence of k_{ICT} is described by a single decreasing curve irrespective of solvents. This means that for the present ICT reaction the solvent polarity effect is not observed. This is due to the comparatively small activation energy ($E_a = 4-5$ kJ/mol)[9] unlike the TICT reaction of 4,4′-diaminodiphenyl sulfone (DAPS) ($E_a = 8-11$ kJ/mol).[7]

TABLE 1: Power-Law Parameter α in $k_{ICT} = A\eta^{-\alpha}$ [a]

	α		
solvent	DMATP	DAPS[b]	AMDMA[c]
ethanol	0.7 (0.71)[d]		
1-propanol	(0.44)	0.44	0.68
1-butanol	0.3 (0.31)	0.29	
1-pentanol	0.3 (∼0.2)	0.24 (0.2)	0.10−0.2

[a] Values in parentheses were determined from the yiel-ratio data. [b] Reference 7. [c] Reference 20. [d] Reference 9.

The empirical power law expression is used to express the viscosity dependence of k_{ICT}

$$k_{ICT} = A\eta^{-\alpha} \qquad (4)$$

where A is a viscosity independent constant and the exponent α can be used as a measue of solvent viscosity dependence. The curve in Figure 1 indicates that the exponent α decreases with increasing η. The α values, which were calculated by assuming an approximate linear dependence for each alcohol, are given in Table 1. The present results agree well with those obtained previously from yield−ratio measurements.[9] This agreement demonstrates the assumption that the variation of the yield ratio (Φ_{ICT}/Φ_{LE}) with pressure exclusively reflects the change of the ICT formation rate. Namely, the deactivation rate constant of the ICT state is relatively insensitive to pressure. In Table 1, the previous results for the TICT state formation of DAPS[7] and 4-(9-anthrylmethyl)-*N*,*N*-dimethylaniline (AMDMA)[20] are included for comparison.

In order to understand such decreasing behavior of α with increasing viscosity, it is necessary to obtain accurate information of the solvation dynamics. Then, we measured the TDSS of C153 as a function of pressure in the same solvents and compared the ICT rate constant of DMATP with the average solvation time thus obtained. C153 is considered as a representative of rigid solute whose excitation does not involve important changes in specific solute−solvent interactions.[10−14] In addition, this is a completely rigid molecule having only a single low-lying excited singlet state.

Time-Resolved Stokes Shift of C153 and Spectral Solvation Response Function. The time-dependent properties of the emission spectrum are generally quantified in terms of a spectral response function, $C(t)$,[21] defined by

$$C(t) = \frac{\tilde{\nu}(t) - \tilde{\nu}(\infty)}{\tilde{\nu}(0) - \tilde{\nu}(\infty)} \qquad (5)$$

where $\tilde{\nu}(t)$, $\tilde{\nu}(0)$, and $\tilde{\nu}(\infty)$ denote the emission maximum observed at times t, zero, and infinity, respectively. It is this response function that has been used as directly comparable to the theoretical prediction of solvation dynamics, since the experimentally determined $C(t)$ is related to the solvation energy relaxation response function under the proper conditions.[21,22] In the framework of a simple continuum model, in which the polar solvent surrounding the solute molecule is replaced by a uniform dielectric continuum characterized by a frequency-

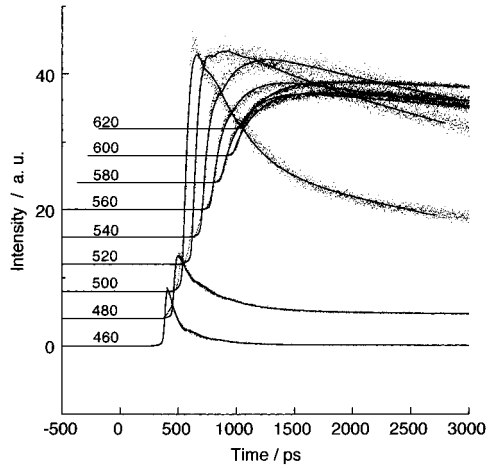

Figure 2. Response curves of C153 at different wavelengths. The solid lines through the data points represent multiexponential fits.

dependent dielectric constant $\epsilon(\omega)$, the decay of $C(t)$ is predicted to be a single-exponential function *i.e.*, $C(t) = A \exp(-t/\tau_L)$, which decays with the longitudinal relaxation time of solvent (τ_L).

The primary data in the time-resolved experiments consist of a set of fluorescence decays recorded at a series of wavelengths for every 10 nm, spanning the steady state fluorescence spectrum between 450 and 650 nm. The interest is to derive from these data the spectral response function $C(t)$ defined by eq 5. The emission decays were fit to eq 1. In general, three exponentials were required for the best fit to the population decay. In Figure 2, examples of emission decays and multiexponential fits of C153 in 1-butanol at 392 MPa are illustrated in 20 nm steps from 460 to 620 nm.

Then the resulting fits were pierced to yield time-resolved spectra from which $C(t)$ can be derived. The decay curve at each wavenumber is normalized so that the integrated value may reproduce the intensity of the steady state emission spectrum at the given wavenumber. The detailed procedure has been described in detail by Maroncelli, Fleming, and co-workers.[12] Typical reconstructed time-resolved emission spectra of C153 in 1-pentanol at 0.1 and 392 MPa are illustrated in Figure 3. In this work a time scale longer than 20 ps is employed. The poor quality of the fit in the time scale faster than 20 ps is due to the incomplete deconvolution of IRF, which has a dramatic impact on the quality of the fits. At the times longer than 20 ps, there are only small changes in the width or shape of the spectrum with time. In Figure 3, the steady state fluorescence spectra are also included. The data shown here are typical of what is observed in all compressed alcohol solvents examined. The spectral evolution involves mainly a time-dependent shift of the spectrum between the limits set by the estimated time-zero and the steady state emission spectra. In order to utilize all of the data points in determining spectral frequencies, each spectrum was fit to a log-normal shape function.[23] As illustrated by the solid curves in Figure 3, log-normal fits provide good representation of the time-resolved data in the time scale longer than 20 ps.

Finally, in order to compute $C(t)$ *via* eq 5, we will use the average of two frequency measures, *i.e.*, the peak frequency, $\nu_m(t)$, which is obtained directly from the log-normal fits, and the centroid of the spectrum, $\nu_c(t)$, which is defined by $\int_0^\infty \nu I(t, \nu)\, d\nu / \int_0^\infty I(t, \nu)\, d\nu$.[23] Typical spectral response functions $C(t)$ in 1-pentanol constructed from such a procedure are shown in Figure 4. We find that the decay time becomes longer as the pressure increases.

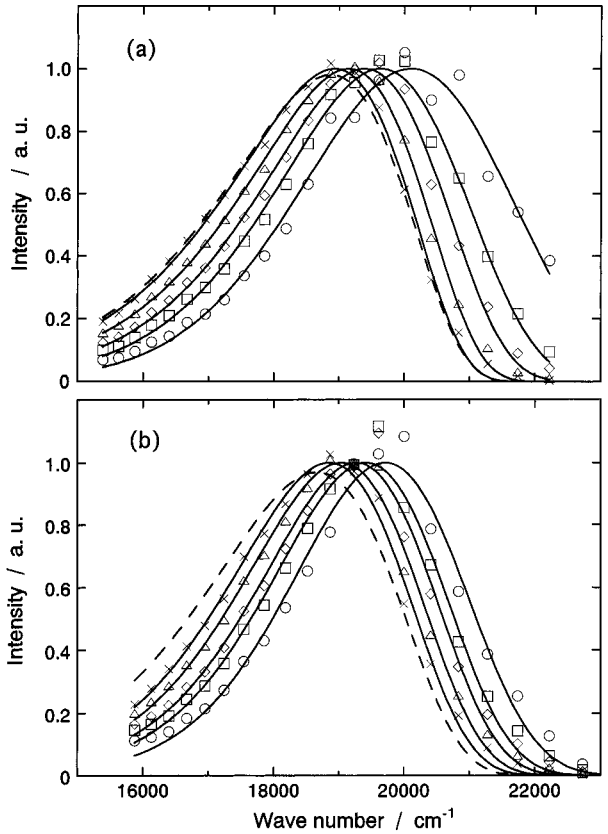

Figure 3. Time-resolved and steady state spectra of C153 in 1-pentanol at (a) 0.1 MPa and (b) 490 MPa. (From blue side: ○, 0 ps; □, 100 ps; ◇, 200 ps; △, 500 ps, X, 1000 ps.) The continuous curves passing through the data points show the log-normal fits to these data. The dashed line denotes the steady state spectrum.

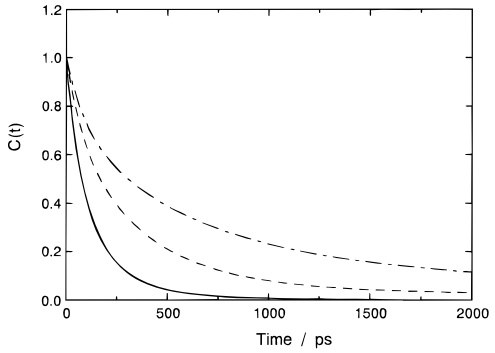

Figure 4. Spectral response function of C153 in 1-pentanol determined by the log-normal fit to the time-resolved spectra (—, 0.1 MPa; – –, 196 MPa; – - –, 392 MPa).

Here, it should be noted that functions $C(t)$ so reproduced are in general not a single-exponential function of time, but they can reasonably be represented by biexponential functions. Therefore, in the following we will use an average time, which is given by the time integral of $C(t)$ as a measure of solvation time.

$$\tau_s = \int_0^\infty C(t)\, dt \tag{6}$$

A summary of solvation time (τ_s) obtained from high-pressure TDSS experiments is provided in Table 2. The fits were performed on data sets logarithmically spaced in time, using several hundred points in every 10 ps step for the time scale longer than 20 ps.

In Figure 5, the resulting high-pressure τ_s values at given viscosities are compared with the longest component of τ_L from

TABLE 2: Average Solvation Times (τ_s) Determined by High-Pressure TDSS Measurements of C153 in Alcohols

	τ_s[a]/ps		
pressure, MPa	1-propanol	1-butanol	1-pentanol
0.1	56 (26)	50 (63)	137 (103)
196	74	185	391
392	557	1324	843

[a] Values in parentheses are from ref 12.

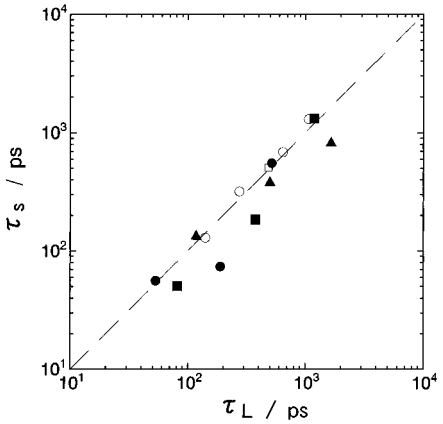

Figure 5. Comparison of τ_s with τ_L (●, 1-propanol; ■, 1-butanol; ▲, 1-pentanol). Open symbols denote the values τ_s determined by low-temperature TDSS measurements[12,26] (○, 1-propanol; □, 1-butanol). The dashed line represents $\tau_s = \tau_L$.

low-temperature sources[24−26] on a logarithmic scale (for τ_L, *vide infra*). The τ_s values determined by low-temperature TDSS measurements for the same probe[12,26] are also included in this figure for comparison. The dashed line in Figure 5 represents $\tau_s = \tau_L$. One finds that there is a good correlation between τ_s and τ_L, even though the $C(t)$ decay is not completely exponential.[27] The time values considered in this comparison span more than 1 order of magnitude; *ca.* 50−1000 ps. From these facts we can conclude that within the time region studied the simple continuum predictions do provide a surprisingly good approximation to the observed solvent relaxation times. Note that in this time scale the solvation dynamics of alcohol are characterized by hydrogen-bonding dynamics in molecular aggregates.[24,25] However, it has also been reported by Maroncelli[28] that the average solvent relaxation times of alcohols which have been determined by the TDSS in various solvents at atmospheric pressure even with the time resolution of ∼1 ps correlate well with the average of three longitudinal relaxation times.

Effect of Solvent Dynamics on k_{ICT}. In Figure 6, the inverse of ICT rate constants (k_{ICT}^{-1}) is compared with τ_s as well as τ_L of given viscosity conditions for the four compressed alcohol solvents. The dashed line in this figure is a line with a slope of unity, which represents perfect agreement between k_{ICT}^{-1} and τ_s or τ_L. Here, the τ_L values are the longest components of the longitudinal relaxation times for alcohols estimated from low-temperature sources,[24−26] since the high-pressure τ_L values are not available. Namely, the τ_L values at given viscosities are obtained from the interpolation of the low-temperature data through polynomial fittings.

The most obvious conclusion to be drawn from the comparison in Figure 6 is that there are two distinct time and viscosity regions. In the lower viscosity less than *ca.* 10 mPa s, k_{ICT}^{-1} correlates with τ_s as well as τ_L. While with increasing the viscosity, k_{ICT}^{-1} shifts toward a value greater than τ_s as well as τ_L. Such behavior can be explained by the shift of reaction path on the excited state free energy surface. Similar to the

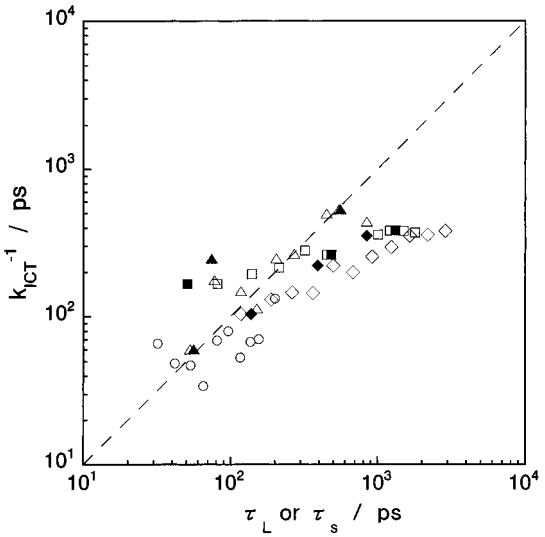

Figure 6. Comparison of k_{ICT}^{-1} with τ_s and τ_L. The dashed line represents $k_{ICT}^{-1} = \tau_s$ or τ_L. Open symbols represent the plot of k_{ICT}^{-1} vs τ_L. Solid symbols represent the plot of k_{ICT}^{-1} vs τ_s. (△, ▲, 1-propanol; □, ■, 1-butanol; ◇, ◆, 1-pentanol).

Sumi−Nadler−Marcus model,[29] the reaction coordinate is divided into two contributions; one is the solvent coordinate, the other is the intramolecular coordinate of nuclear motion. Here, we attempted to simulate the steady state emission spectrum of DMATP using the semiempirical model developed by Barbara and co-workers.[30] According to the result, we find[31] that the present reaction is not in the Marcus inverted region but in the normal region unlike the ICT of 4-(9-anthryl)-*N*,*N*-dimethylaniline (ADMA).[32] Therefore, we can draw a figure of the S_1 state potential energy surface, which has been illustrated in Figure 6 of ref 9.

In the low viscosity regime (*I*), where the solvent relaxation is faster than the solute reactive motion, where $k_{ICT} \ll \tau_s^{-1}$, the orientation of the solvent dipoles around the solute molecules is fast enough to keep up with the change of charge distribution of the ICT process in the excited state. Conversely, in the high viscosity regime (II), where $k_{ICT} \ll \tau_s^{-1}$, the solvent dipoles move much slower than the reactive solute motion such that the orientation of the solvent dipoles does not change at all before the reaction is completed. This extreme can be characterized by the nonrelaxed reaction path where the molecule starts at the Franck−Condon state (F), which is determined by the solvent shell dipoles corresponding to the charge distribution in the ground state. In the intermediate viscosity region between the two limiting regimes, where $k_{ICT} \approx \tau_s^{-1}$, the relaxation of the solvent dipole orientation controls the reaction dynamics. In this case the survival decay of the LE state should exhibit a multiexponential function, while in the case of pure I or II schemes the decay should be a single-exponential function. The fact that the decay curve of the highest pressure in the present result cannot be represented by the single-exponential form may indicate that the reaction path does not attain the completely pure II path at this viscosity condition.

Therefore, we can conclude that with increasing solvent viscosity by application of pressure, the reaction path shifts from the solvation−controlled scheme to the path controlled by intramolecular vibrational motion. It is this behavior that has been called as "pressure tuning effect" of the solvent viscosity, which has previously been described for the TICT formation of DAPS.[8]

For the verification of solvent viscosity dependence, the size effect of substituent alkyl groups, which are the twisting moiety of the TICT reaction in DMABN and other related TICT state

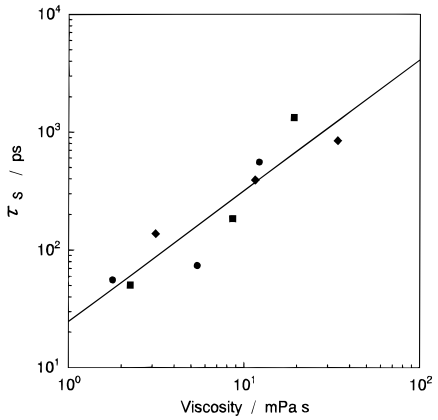

Figure 7. Viscosity dependence of τ_s (●, 1-propanol; ■, 1-butanol; ▲, 1-pentanol). The solid line represents the fit to $\tau_s \propto \eta^{\alpha}$ with $\alpha = 1.1$.

forming molecules, has often been examined so far.[5] However, as stated above, if the reaction is in the solvent relaxation controlled regime, k_{ICT} is naturally invariant with the size of dialkyl group. Namely, it is not the solute motion but the solvent low-frequency relaxational motion that determines the rate of the ICT reaction in this regime.

It should be noted that in the highest viscosity regime at high pressures where the low-frequency solvent motion is almost frozen, the power-law parameter approaches ~0.3 for the ICT reaction of DMATP. In the case of DAPS,[7] it is as small as ~0.2. This value may indicate the intrinsic dynamic solvent effect for the barrier crossing process which is dependent on high-frequency solvent motion, while the low-frequency solvent relaxational motion is frozen. This is too weak a viscosity dependence to be provided by the Kramers model for the dynamic solvent effect.[33]

By assuming a planar ground state geometry, results from gas phase spectroscopy and CNDO calculations of photoionization spectra of DMABN have shown[34] that the equilibrium geometry of the LE state and the crossing from the LE to ICT state at constant solvent polarity locate at a twist angle of 30° and 70°, respectively. Only a small twisting motion of 40° is needed. Namely, a rotation of the dialkylamino group to the perpendicular geometry is not required to enable the ICT to occur. These calculations may substantiate that viscosity effects on the formation of the TICT state of DMABN might be smaller than that originally expected.[6]

Finally, we can realize that such a "pressure tuning effect" is originally produced by a large viscosity dependence of τ_s. Figure 7 shows the plot of τ_s against solvent viscosity in double-logarithmic scale. The slope amounts to 1.1. The viscosity dependence of solvent relaxation is much stronger than that of the ICT process. This behavior is considered as a specific character of alcohol solvent having hydrogen bonding.

Summary and Conclusions

In this paper we have reported the dynamic solvent effect on the ICT reaction of DMATP in alcohols by means of a high-pressure method. In order to describe the solvation effect on the reaction, the solvent relaxation times (τ_s) at high pressures have been determined by measuring the TDSS of C153 in compressed alcohol solvents.

The high-pressure τ_s values thus obtained at given viscosities correlate well with the longest τ_L values estimated from low-temperature sources. This indicates that in the present time regime with a resolution of ~10 ps the continuum model adequately provides the solvent response.

When k_{ICT}^{-1} are compared with τ_s (or τ_L), it is found that the excited potential needs to be described as a two-dimensional surface, taking into account the low-frequency solvent relaxational motion and the intramolecular twisting motion. According to the simple simulation of emission spectrum, we find that the ICT reaction of DMATP is not in the Marcus inverted region. It follows that the reaction scheme can be described on a two-dimensional potential in the excited state (*cf.* Figure 6 in ref 9).

The so-called "pressure tuning effect" of solvent relaxation time has been verified for the ICT reaction of DMATP in alcohol solutions. Namely, it has been established in this paper that the previous discussions,[8,9] which have been made by using the longest τ_L values of alcohols from low-temperature sources as a measure of solvation time scale, are completely correct. The relative importance of solvation dynamics and intramolecular nuclear motion in determining the reaction dynamics is dependent on the relative time scales of these molecular motions on the excited state potential and its shape.

Not only for the present ICT reaction of DMATP but also for the TICT reaction of DAPS[8] and AMDMA[20] (*cf.* Table 1) the power-law parameter α decreases to 0.2−0.3 in a high viscosity regime at high pressures. This value is considered as reflecting the intrinsic barrier crossing dynamics, which is controlled by high-frequency solvent motion such as a rotation of the hydroxyl group of the alcohol. Such small viscosity dependence in DMATP may support the conclusion that the amplitude of the intramolecular twisting motion is not so large, which has been suggested by computational works.[34]

In addition, it should be noted that such weak viscosity dependence would be observed only by the high-pressure method. Further advances in these areas would be anticipated by studying the perturbation of external pressure to understand the detailed role of solvent dynamics to the ICT reaction kinetics.

References and Notes

(1) Hynes, J. T. *Ultrafast Dynamics of Chemical Systems*; Simon, J. D., Ed.; Kluwer; Dordrecht, 1994; p 345.

(2) Barbara, P. F.; Jarzeba, W. *Adv. Photochem.* **1990**, *15*, 1. Simon, J. D. *Pure Appl. Chem.* **1990,** *62*, 2243. Maroncelli, M.; MacInnis, J.; Fleming, G. R. *Science* **1989**, *243*, 1674. Bagchi, B. *Ann. Rev. Phys. Chem.* **1989**, *40*, 115.

(3) Lippert, E.; Rettig, W.; Bonacis-Koutecky, V.; Heisel, F.; Miehe, J. A. *Adv. Chem. Phys.* **1987**, *68*, 1. Rettig, W. *Modern Models of Bonding and Delocalization*; Liebman, J. F., Greeberg, A., Eds.; VCH Publishers: 1988; Chapter 5, p 229 and references cited therein.

(4) Hicks, J. M.; Vandersall, M. T.; Babarogic, Z.; Eisenthal, K. B. *Chem. Phys. Lett.* **1985**, *116*, 18.

(5) Simon, J. D.; Su, S.-G. *J. Phys. Chem.* **1990**, *94*, 3656. Simon, J. D.; Doolen, R. *J. Am. Chem. Soc.* **1992**, *114*, 4861.

(6) Grabowski, Z. R.; Rotkiewicz, K.; Siemiarczuk, A.; Cowley, D. J.; Baumann, W. *Nouv. J. Chim.* **1979**, *3*, 443.

(7) Bulgarevich, D. S. Kajimoto, O.; Hara, K. *J. Phys. Chem.* **1995**, *99*, 13356.

(8) Hara, K.; Bulgarevich, D. S.; Kajimoto, O. *J. Chem. Phys.* **1996**, *104*, 9431.

(9) Hara, K.; Kometani, N.; Kajimoto, O. *J. Phys. Chem.* **1996**, *100*, 1488.

(10) Castner, E. W., Jr.; Maroncelli, M.; Fleming, G. R. *J. Chem. Phys.* **1987**, *86*, 1090.

(11) Su, S.-G.; Simon, J. D. *J. Phys. Chem.* **1987**, *91*, 2693. Simon, J. D.; Su, S.-G. *Chem. Phys.* **1991**, *152*, 143.

(12) Horng, M. L.; Gardecki, J. A.; Papazyan, A.; Maroncelli, M. *J. Phys. Chem.* **1995**, *99*, 17311. Maroncelli, M.; Fleming, G. R. *J. Chem. Phys.* **1987**, *86*, 6221; **1990**, *92*, 3251.

(13) Jarzeba, W.; Walker, G. C.; Johnson, A. E.; Barbara, P. F. *Chem. Phys.* **1991**, *152*, 57. Kahlow, M. A.; Jarzeba, W.; Kang, J. T. Barbara, P. F. *J. Chem. Phys.* **1989**, *90*, 151. Jarzeba, W.; Walker, G. C.; Johnson, A. E.; Kahlow, M. A. *J. Phys. Chem.* **1988**, *92*, 7039. Kahlow, M. A.; Kang, T. J.; Barbara, P. F. *J. Chem. Phys.* **1988**, *88*, 2372.

(14) Chapman, C. F.; Fee, R. S.; Maroncelli, M. *J. Phys. Chem.* **1995**, *99*, 4811; **1991**, *94*, 4929. Fee, R. S.; Milson, J. A.; Maroncelli, M. *J. Phys. Chem.* **1990**, *95*, 5170. Chapman, C. F.; Maroncelli, M. *J. Phys. Chem.* **1991**, *95*, 9095.

(15) Hara, K.; Morishima, I. *Rev. Sci. Instrum.* **1988**, *59*, 2397.
(16) Hara, K.; Kometani, N.; Kajimoto, O. *Chem. Phys. Lett.* **1994**, *225*, 381.
(17) The decay time of the $S_1 \rightarrow S_0$ deactivation becomes shorter as pressure increases. See, for example; Offen, H. *Organic Molecular Photophysics*; Birks, J. B., Ed.; John Wiley & Sons: New York, 1973; p 103.
(18) Bridgman, P. W. *Collected Experimental Papers*, Vol. IV; Harvard University Press: Cambridge, MA, 1964; p 2043.
(19) Matsuo, S.; Makita, T. *Int. J. Thermophys.* **1989**, *10*, 833.
(20) Bulgarevich, D. S. Dr. Thesis, Kyoto University, 1996.
(21) Bagchi, B.; Oxtoby, W.; Fleming, G. R. *Chem. Phys.* **1984**, *86*, 257.
(22) van der Zwan, G.; Hynes, J. T. *J. Phys. Chem.* **1985**, *89*, 4181.
(23) Fraser, R. D. B.; Suzuki, E. *Spectral Analysis*; Blackburn, J. A., Ed.; Marcel Dekker: New York, 1970; p 171.
(24) For linear alcohols, it has been noted[25] that the dielectric response is described by a sum of three regions of Debye dispersion. Here, we adopted the longest component, which is associated with the time scale of hydrogen-bonding dynamics in molecular aggregates.
(25) Garg, S. K.; Smyth, C. P. *J. Phys. Chem.* **1965**, *69*, 1294.
(26) Su, S.-G.; Simon, J. D. *Chem. Phys. Lett.* **1989**, *158*, 423. Su, S.-G.; Simon, J. D. *J. Chem. Phys.* **1988**, *89*, 908.
(27) The effect of inhomogeneous decay kinetics on dynamic spectral shift in the fast time region might contribute to $C(t)$ and lead to a distorted representation of the solvation dynamics. *Cf.* Agmon, N. *J. Phys. Chem.* **1990**, *94*, 2959.
(28) Maroncelli, M. *J. Mol. Liq.* **1993**, *57*, 1.
(29) Sumi, H.; Marcus, R. A. *J. Chem. Phys.* **1986**, *84*, 4894. Nadler, W.; Marcus, R. A. *J. Chem. Phys.* **1987**, *86*, 3906.
(30) Kang, T. J.; Jarzeba, W.; Barbara, P. F.; Fonseca, T. *Chem. Phys.* **1990**, *149*, 81. Kang, T. J.; Kahlow, M. A.; Giser, D.; Swallen, S.; Nagarajan, V.; Jarzeba, W.; Barbara, P. F. *J. Phys. Chem.* **1988**, *92*, 6800.
(31) Kometani, N. Dr. Thesis, Kyoto University, 1997. The three parameters varied are the exothermicity ($\Delta G°$), the force constant (k_s, assumed to be the same for all states), and the mixing matrix element between LE and ICT states (H_{int}). The values for $\Delta G°$, k_s, and H_{int} used for the best simulation are 12.8, 218, and 29.3 kJ/mol, respectively.
(32) Tominaga, K.; Walker, G. C.; Jarzeba, W.; Barbara, P. F. *J. Phys. Chem.* **1991**, *95*, 10475.
(33) Kramers, H. A. *Physica* **1940**, *7*, 284.
(34) Warren, J. A.; Bernstein, E. R.; Seeman, J. I. *J. Chem. Phys.* **1988**, *88*, 871. Grassian, V. H.; Warren, J. A.; Bernstein, E. R. *J. Chem. Phys.* **1989**, *90*, 3994.